

SUPPORTING INFORMATION

Single-molecule magnet behavior in heterolopetic Dy³⁺ chloro-diazabutadiene complexes: influence of the nuclearity and ligand redox state.

Jérôme Long*,^a Aleksei O. Tolpygin,^b Anton V. Cherkasov,^b Konstantin A. Lyssenko,^{c,d} Yannick Guari^a, Joulia Larionova^a and Alexander A Trifonov*^{b,c}

^a ICGM, Univ. Montpellier, CNRS, ENSCM, Montpellier, France.

^bInstitute of Organometallic Chemistry of Russian Academy of Sciences, 49 Tropinina str., GSP-445, 603950, Nizhny Novgorod, Russia. E-mail: trif@iomc.ras.ru

^cInstitute of Organoelement Compounds of Russian Academy of Sciences, 28 Vavilova str., 119334, Moscow, Russia.

^d. M.V. Lomonosov Moscow State University, Chemistry Department, Leninskie Gory 1, Build 3, Moscow 119991, Russia.

TABLE OF CONTENTS

Figure S1: Perspective view of the crystal packing for 1 and 2 along the <i>b</i> and <i>a</i> crystallographic axes, respectively. Hydrogen atoms have been omitted for clarity.....	4
Figure S2: Perspective view of the crystal packing for 3 and 4 along the <i>a</i> crystallographic axes. Hydrogen atoms have been omitted for clarity.....	5
Figure S3: Frequency dependence of the in-phase (χ') and out-of phase (χ'') susceptibilities for 1- 4 under a zero dc-field.....	6
Figure S4: Temperature dependence of χ' and χ'' for 1-4 for different frequencies under a zero dc-field.....	7
Figure S5: Cole-Cole (Argand) plot obtained using the ac susceptibility data for 1-4 (0 Oe). The solid lines correspond to the best fit with a generalized Debye model or with a sum of two Debye functions. ⁵	8
Figure S6: Frequency dependence of the in-phase (χ') and out-of phase (χ'') susceptibilities for 1- 4 under various dc fields.....	9
Figure S7: Field dependence of the relaxation time for 4 (2 K). The red line represents the fit with Eq. 3.....	10
Figure S8: Frequency dependence of the in-phase (χ') and out-of phase (χ'') susceptibilities for 1-4 under the corresponding dc-fields.	11
Figure S9: Cole-Cole (Argand) plot obtained using the ac susceptibility data for 1-4 under the corresponding dc fields. The solid lines correspond to the best fit with a generalized Debye model or with a sum of two Debye functions.....	12
Figure S10: Orientation of the anisotropic axis (purple) in 1-2 obtained from the MAGELLAN software. ¹	13
Figure S11: Orientation of the anisotropic axis (purple) in 3 obtained from the MAGELLAN ¹ software and considering different negative charge values on the atoms of the NCCN fragment....	14
Figure S12: Orientation of the anisotropic axis (purple) in 4 obtained from the MAGELLAN software. ¹	15
Table S1. Crystal Data and Structure Refinement Details for Complexes 1-4	16
.....	16
Table S2. SHAPE analysis for compounds 1-3.....	16
Table S3. Fitting of the Cole-Cole plots with a sum of two generalized Debye functions under a zero dc-field for 1 in the temperature range 1.8-3.4 K.	17
Table S4. Fitting of the Cole-Cole plots with a sum of two generalized Debye functions under a zero dc-field for 1 in the temperature range 4.2-5.8 K.	17
Table S5. Fitting of the Cole-Cole plots with a generalized Debye model under a zero dc field for 3.	17
Table S6. Fitting of the Cole-Cole plots with a generalized Debye model under a zero dc field for 4.	18

Table S7: Fit parameters of the temperature dependence of the relaxation time for 1 from a combination of Raman and QTM process (zero field) or Raman (1000 Oe).	18
Table S8:Fit parameters of the field dependence of the relaxation time at 15 K for 4.....	18
Table S9. Fitting of the Cole-Cole plots with a sum of two generalized Debye functions under a 1000 Oe dc-field for 1.	18
Table S10. Fitting of the Cole-Cole plots with a sum of two generalized Debye functions under a 1000 Oe dc-field for 4.	19
References	19

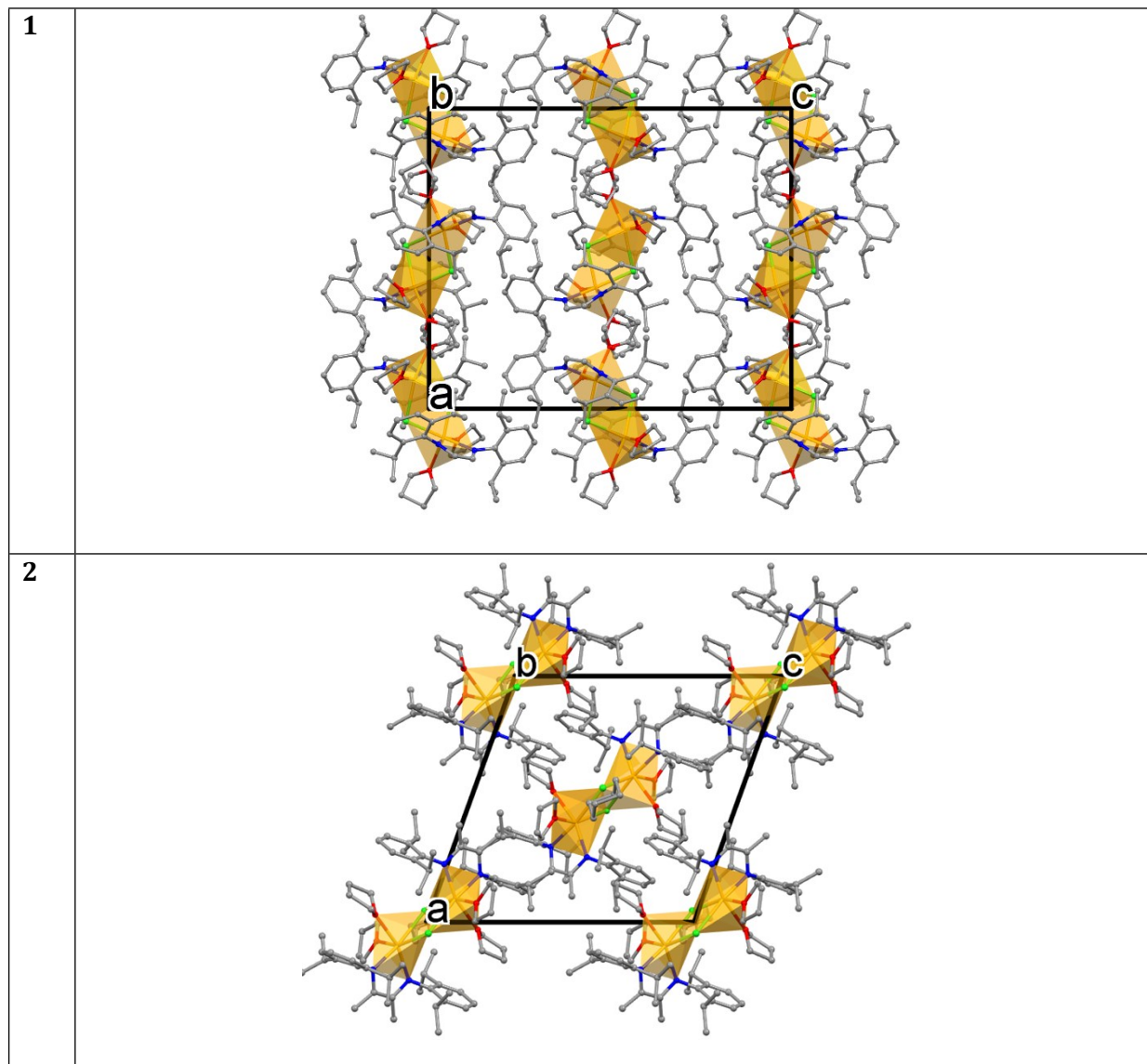


Figure S1: Perspective view of the crystal packing for **1** and **2** along the *b* and *a* crystallographic axes, respectively. Hydrogen atoms have been omitted for clarity.

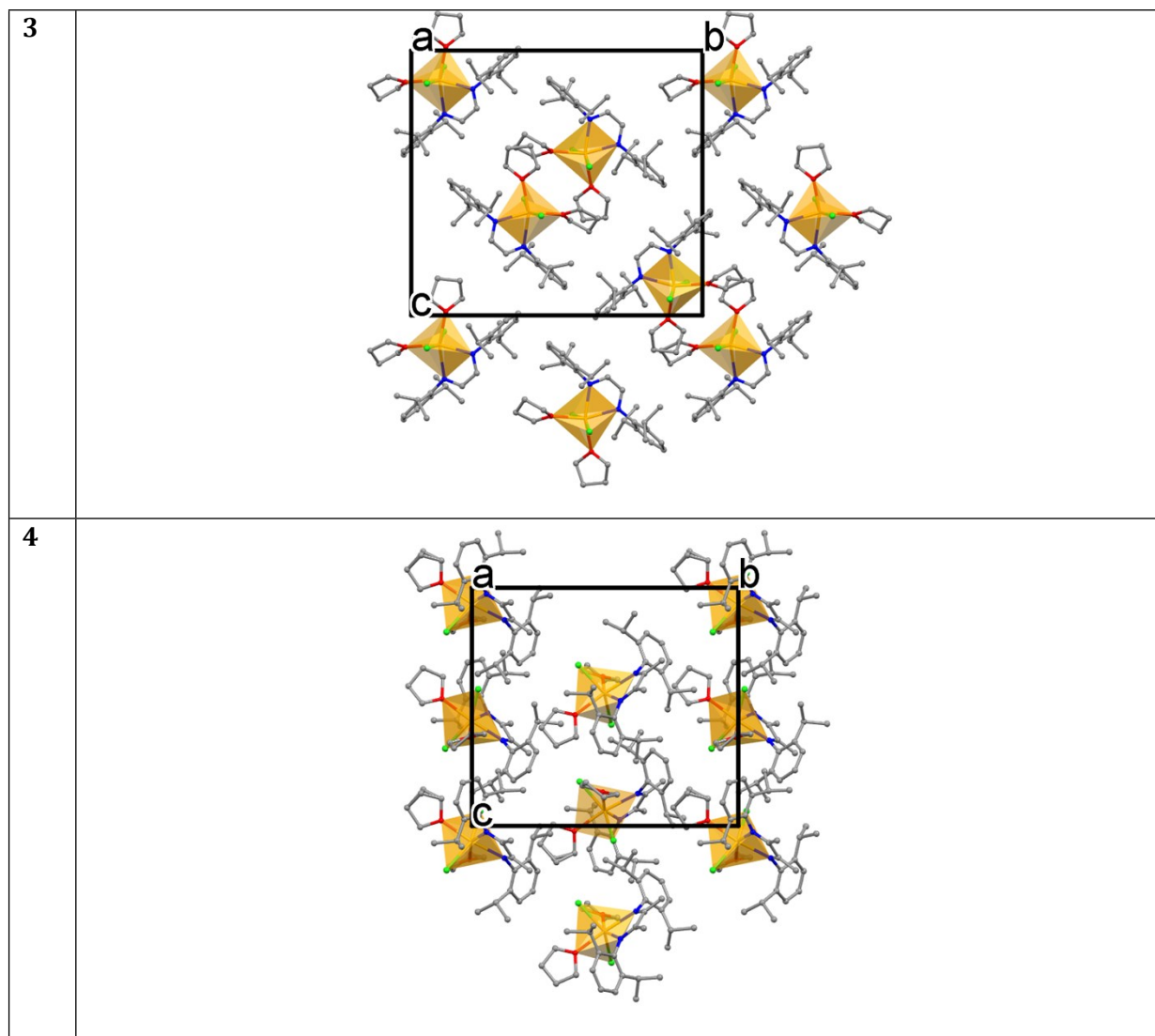


Figure S2: Perspective view of the crystal packing for **3** and **4** along the *a* crystallographic axes. Hydrogen atoms have been omitted for clarity.

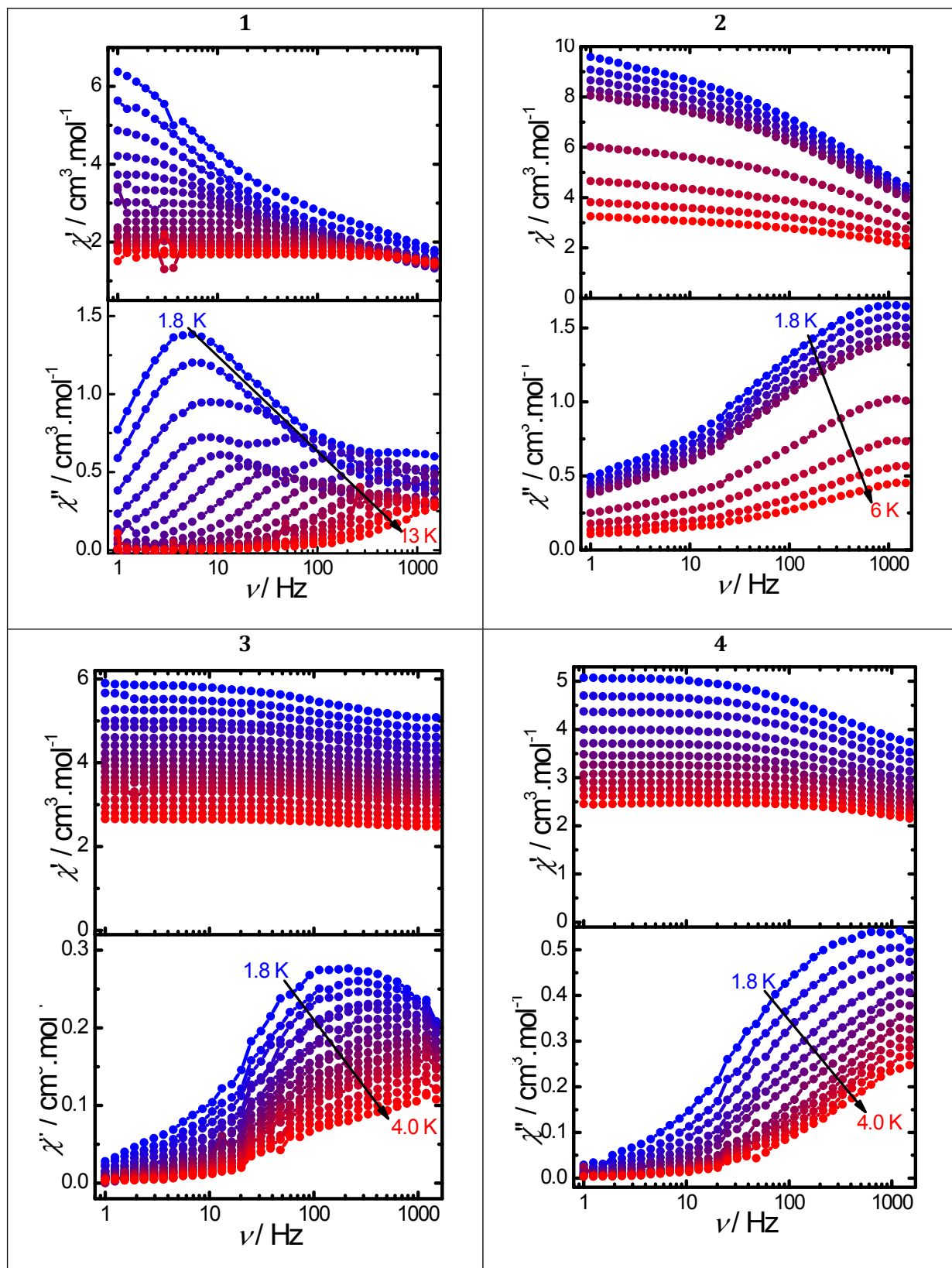


Figure S3: Frequency dependence of the in-phase (χ') and out-of phase (χ'') susceptibilities for **1- 4** under a zero dc-field.

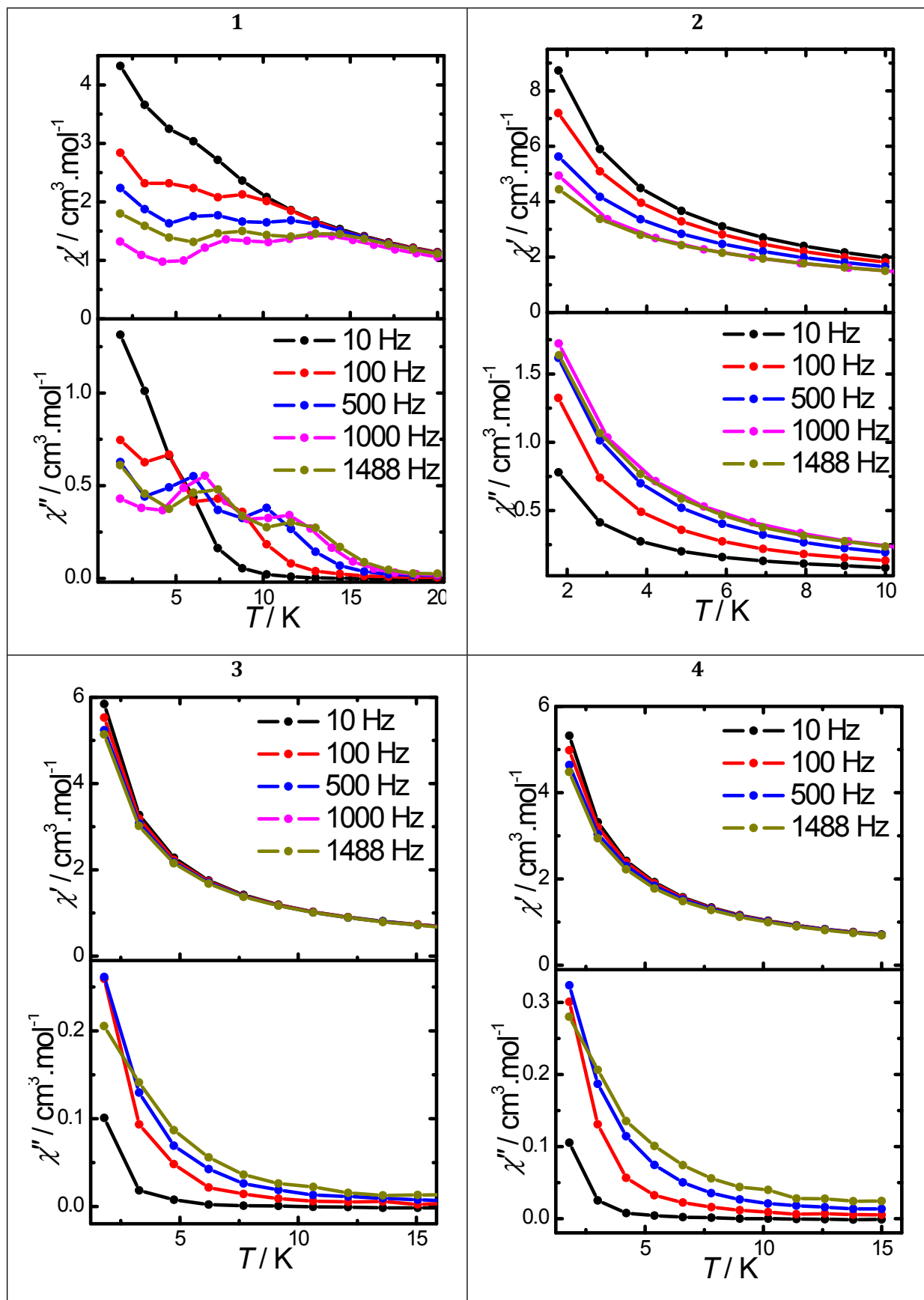


Figure S4: Temperature dependence of χ' and χ'' for **1-4** for different frequencies under a zero dc-field.

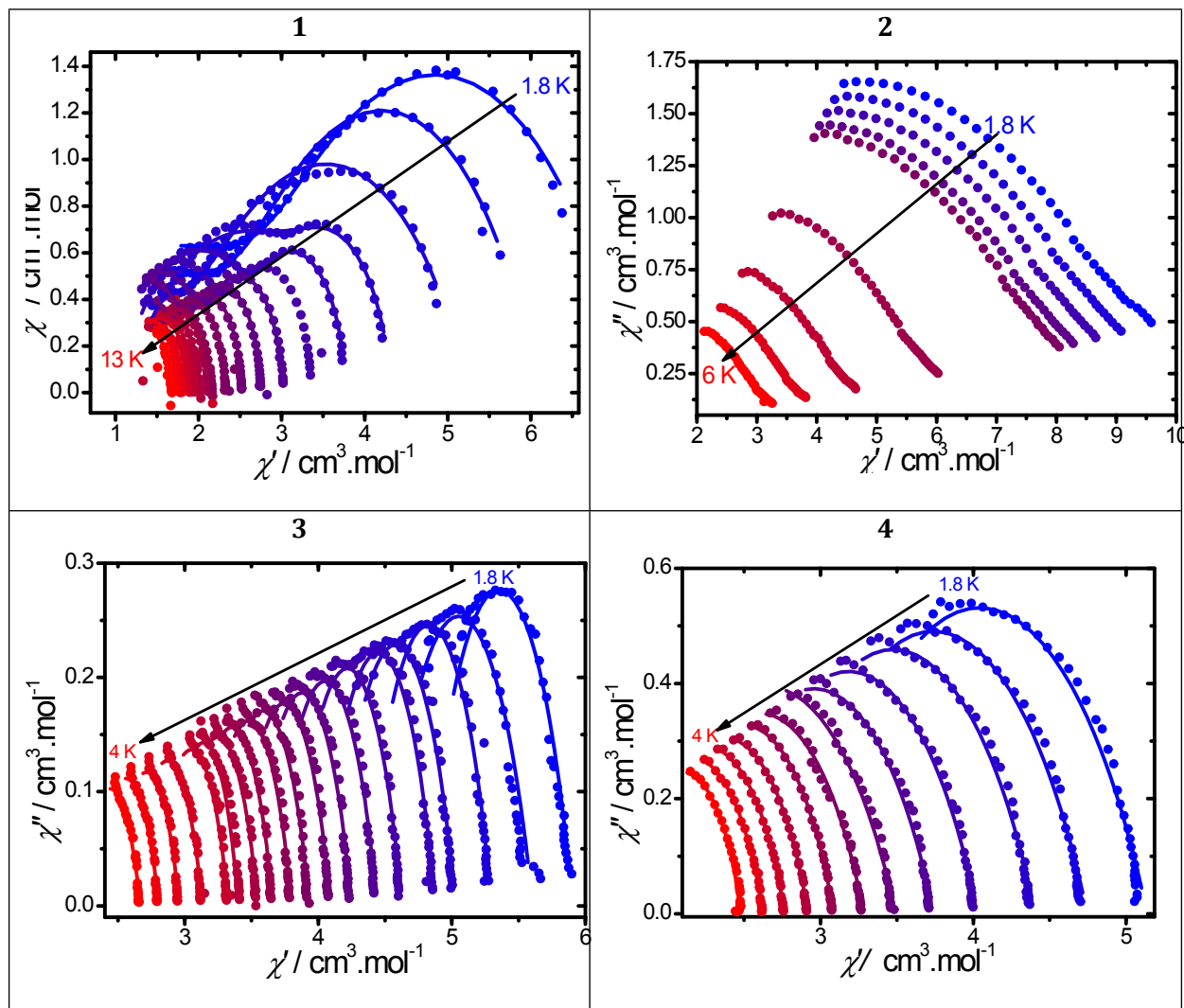


Figure S5: Cole-Cole (Argand) plot obtained using the ac susceptibility data for **1-4** (0 Oe). The solid lines correspond to the best fit with a generalized Debye model or with a sum of two Debye functions.⁵

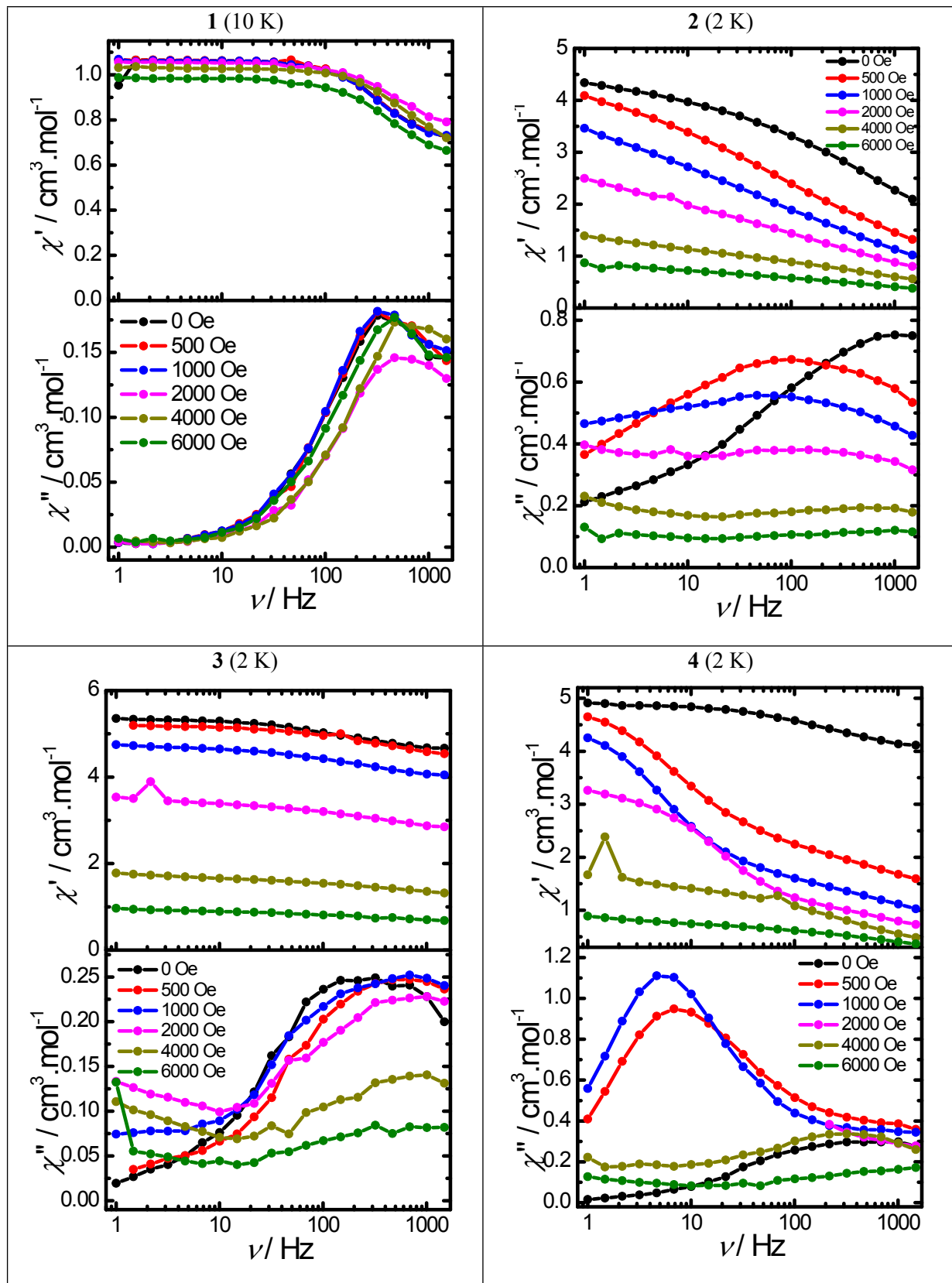


Figure S6: Frequency dependence of the in-phase (χ') and out-of phase (χ'') susceptibilities for 1- 4 under various dc fields.

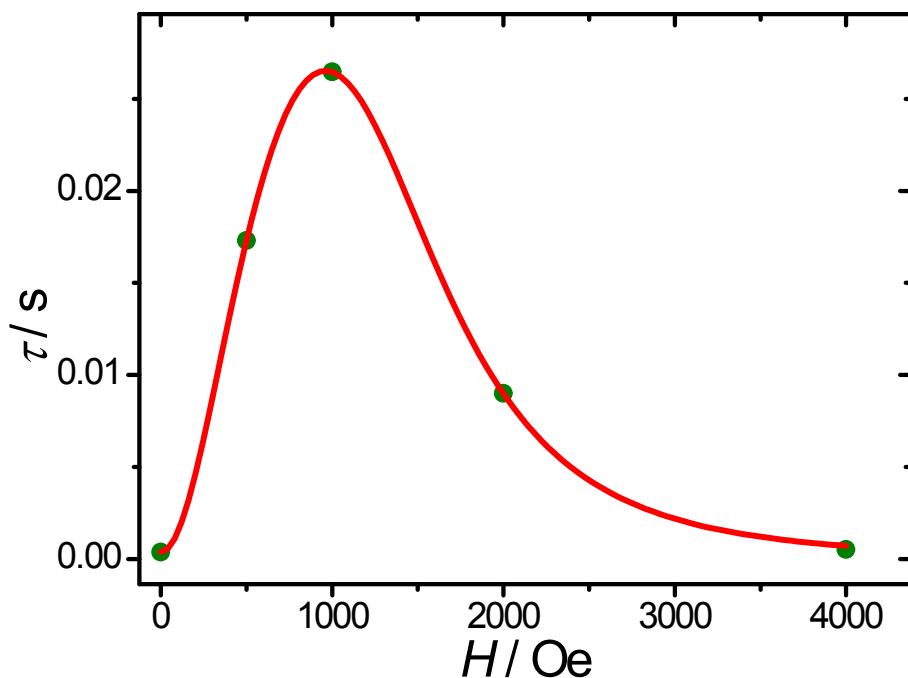


Figure S7: Field dependence of the relaxation time for **4** (2 K). The red line represents the fit with Eq. 3.

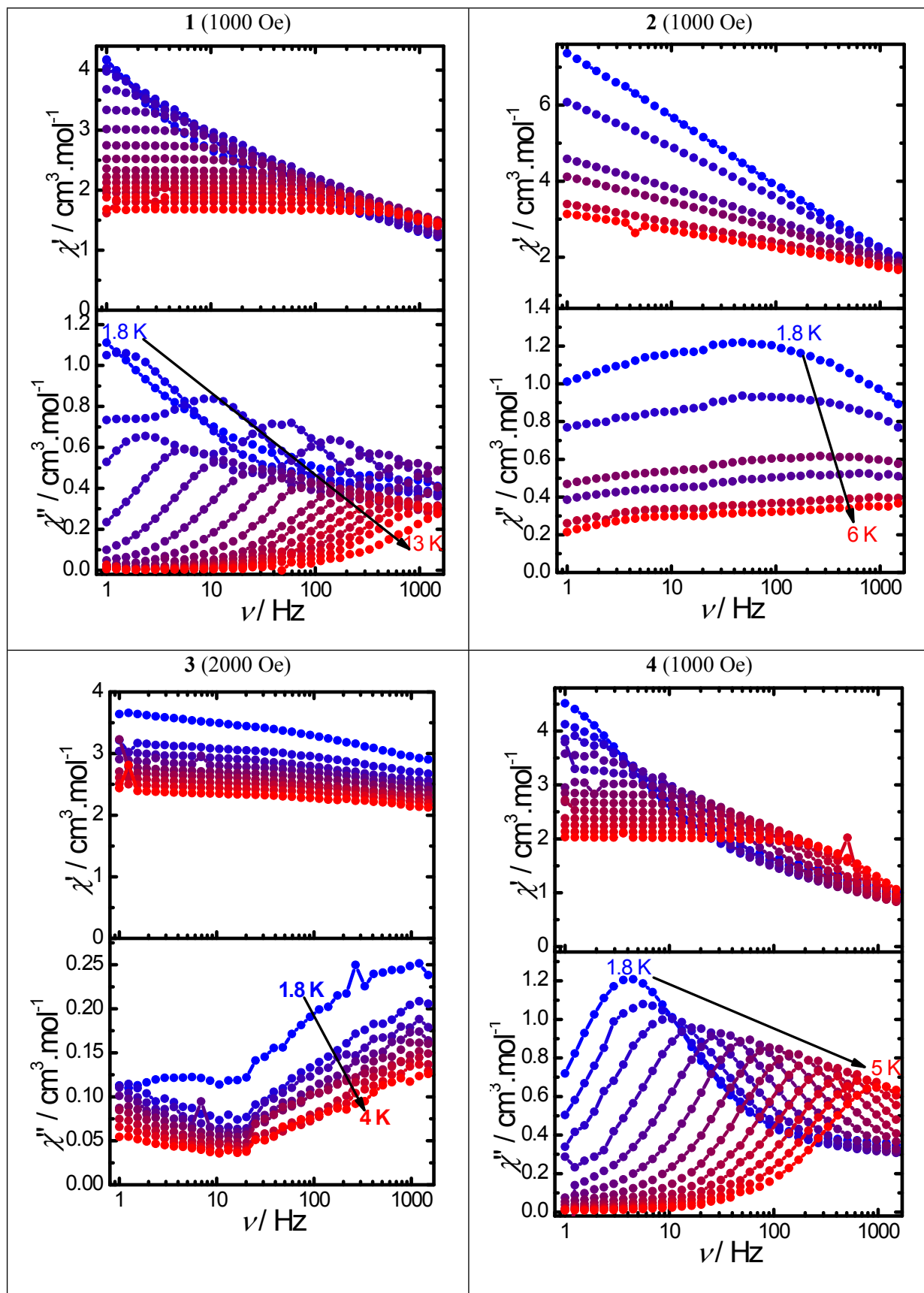


Figure S8: Frequency dependence of the in-phase (χ') and out-of phase (χ'') susceptibilities for **1-4** under the corresponding dc-fields.

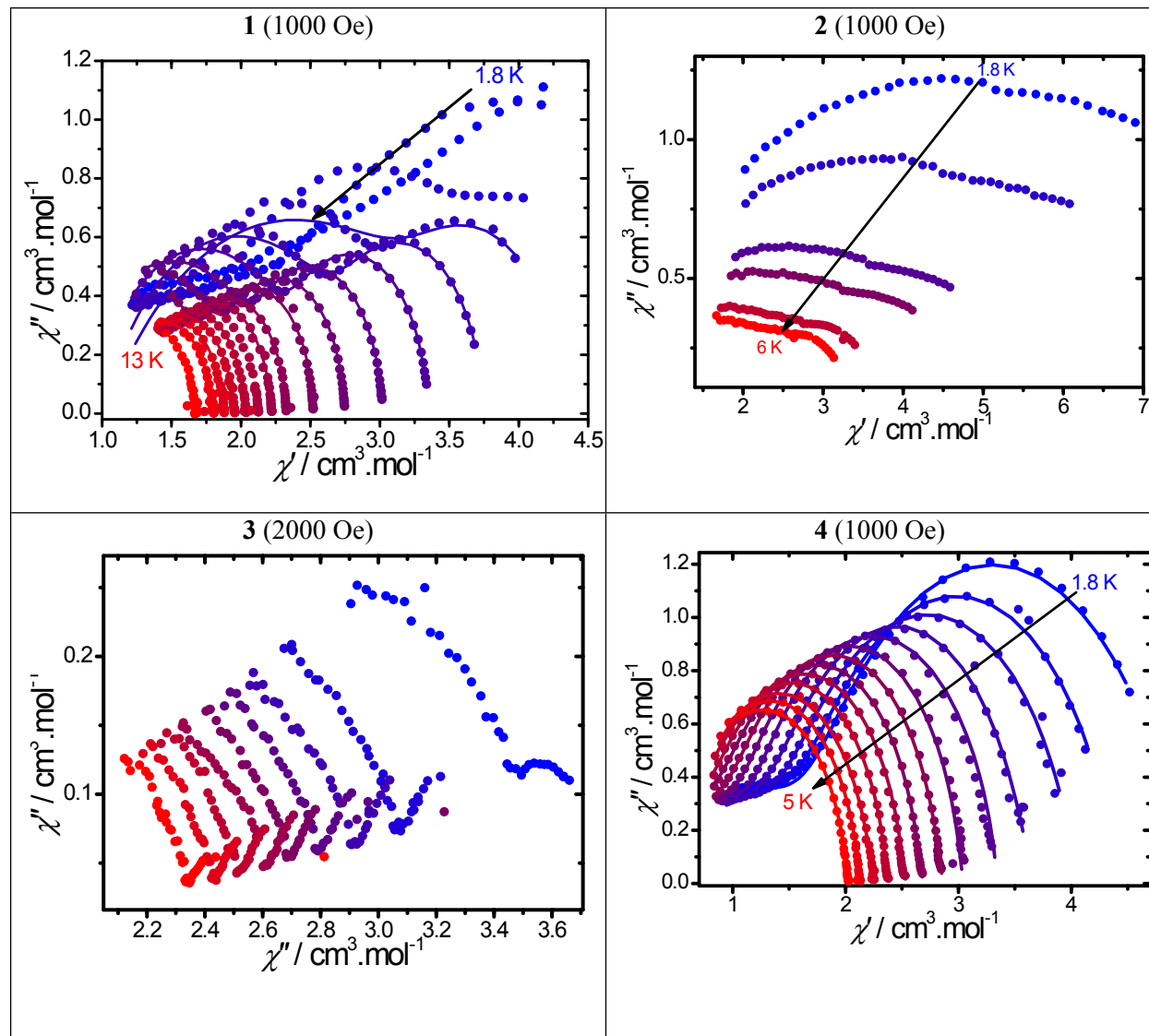


Figure S9: Cole-Cole (Argand) plot obtained using the ac susceptibility data for **1-4** under the corresponding dc fields. The solid lines correspond to the best fit with a generalized Debye model or with a sum of two Debye functions.

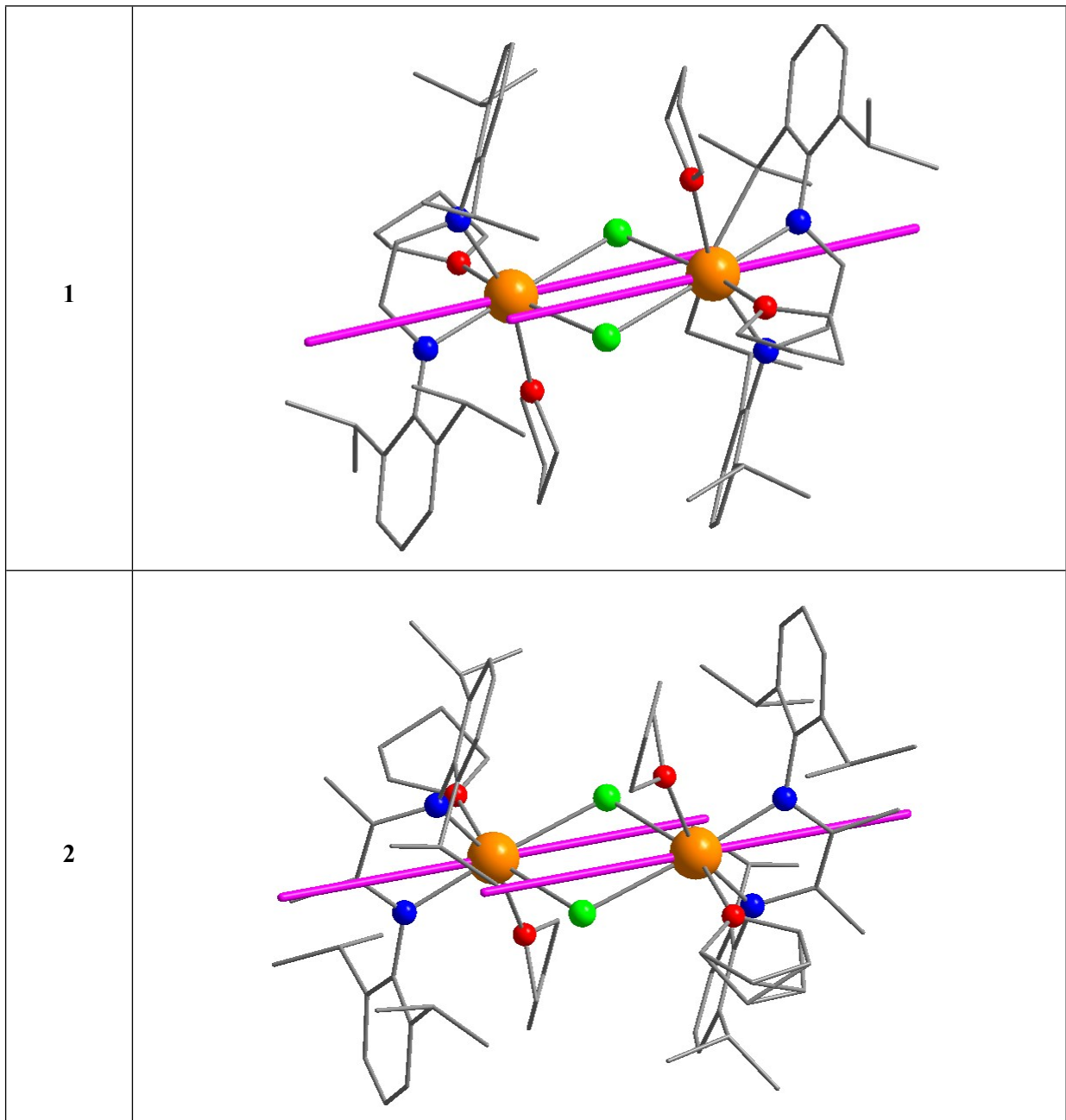


Figure S10: Orientation of the anisotropic axis (purple) in **1-2** obtained from the MAGELLAN software.¹

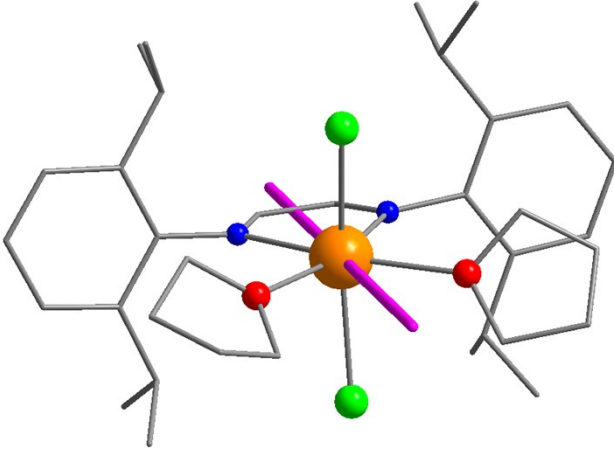
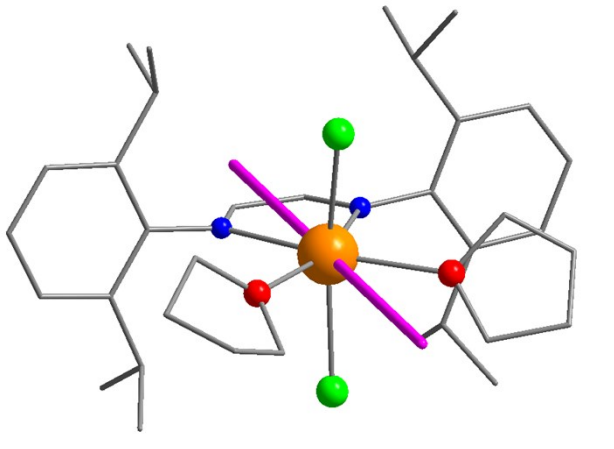
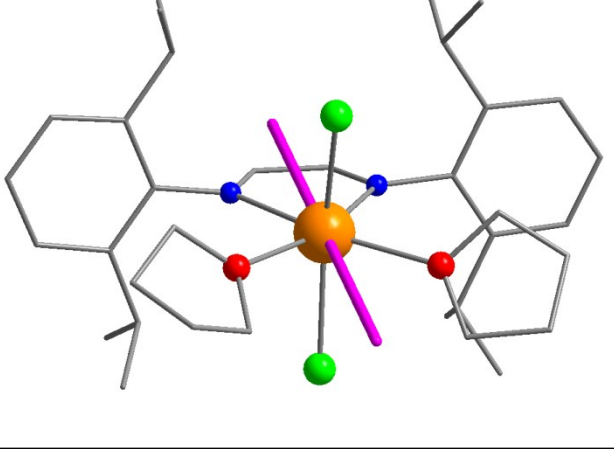
	N1	C1	C2	N2	Orientation
	-1/4	-1/4	-1/4	-1/4	
3	-3/8	-1/8	-1/8	-3/8	
	-4/10	-1/10	-1/10	-4/10	

Figure S11: Orientation of the anisotropic axis (purple) in **3** obtained from the MAGELLAN¹ software and considering different negative charge values on the atoms of the NCCN fragment.

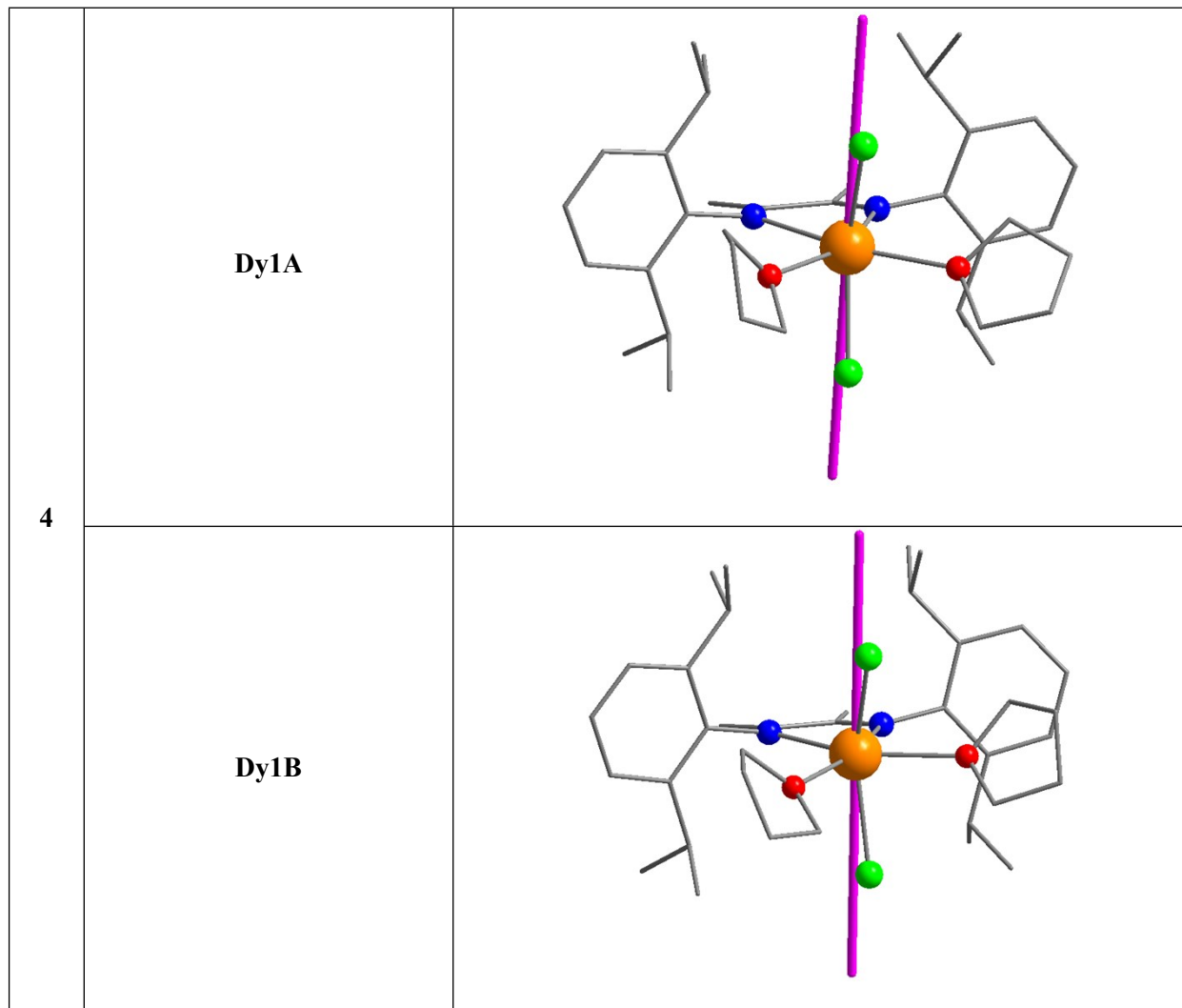


Figure S12: Orientation of the anisotropic axis (purple) in **4** obtained from the MAGELLAN software.¹

Table S1. Crystal Data and Structure Refinement Details for Complexes **1-4**

	1	2	3	4
Empirical formula	C ₆₈ H ₁₀₄ Cl ₂ Dy ₂ N ₄ O ₄	C ₇₂ H ₁₁₂ Cl ₂ Dy ₂ N ₄ O ₄ , ½C ₄ H ₈ O	C ₃₄ H ₅₂ Cl ₂ DyN ₂ O ₂	C ₃₆ H ₅₅ Cl ₂ DyN ₂ O ₂
Formula Weight	1437.45	1529.60	754.17	781.22
T, K	100(2)	120(2)	120(2)	120(2)
Crystal System	Orthorhombic	Monoclinic	Monoclinic	Monoclinic
Space Group	Pbca	P2 ₁ /n	P2 ₁ /n	P2 ₁
Unit Cell Dimensions	a = 19.2467(7) Å b = 15.3525(5) Å c = 23.2322(8) Å α = 90° β = 90° γ = 90°	a = 15.3844(6) Å b = 16.0197(7) Å c = 15.8221(7) Å α = 90° β = 109.7810(10)° γ = 90°	a = 10.1402(6) Å b = 19.7105(10) Å c = 18.5480(10) Å α = 90° β = 105.4108(12)° γ = 90°	a = 13.6988(2) Å b = 17.3825(3) Å c = 15.4968(3) Å α = 90° β = 90.143(2)° γ = 90°
V, Å ³	6864.8(4)	3669.3(3)	3573.9(3)	3690.08(11)
Z	4	2	4	4
d _{calc} , g/cm ³	1.391	1.384	1.402	1.406
μ, mm ⁻¹	2.285	2.142	2.270	2.201
F ₀₀₀	2952	1580	1544	1604
Crystal Size, mm	0.57 × 0.38 × 0.18	0.43 × 0.23 × 0.20	0.32 × 0.20 × 0.12	0.50 × 0.32 × 0.31
θ Range for Data Collection, °	2.44–30.03	1.60–30.03	1.54–30.03	2.97–30.03
Index Ranges	-27 ≤ h ≤ 27 -21 ≤ k ≤ 21 -32 ≤ l ≤ 32	-21 ≤ h ≤ 21 -22 ≤ k ≤ 22 -22 ≤ l ≤ 22	-14 ≤ h ≤ 14 -27 ≤ k ≤ 27 -26 ≤ l ≤ 26	-19 ≤ h ≤ 19 -24 ≤ k ≤ 24 -21 ≤ l ≤ 21
Reflns Collected	109 203	46 802	107 359	74 444
Independent Reflns (R _{int})	10 040 (0.0408)	10 734 (0.0459)	10 451 (0.0599)	21 544 (0.0341)
Parameters (Restraints)	425 (70)	455 (78)	386 (0)	804 (1)
Completeness to θ, %	99.9	100.0	100.0	99.8
S(F ²)	1.057	1.009	1.022	1.018
Flack (absolute structure) parameter			0.12(2)	
Final R Indices (I>2σ(I))	R ₁ = 0.0211 wR ₂ = 0.0451	R ₁ = 0.0272 wR ₂ = 0.0559	R ₁ = 0.0224 wR ₂ = 0.0485	R ₁ = 0.0303 wR ₂ = 0.0688
Final R Indices (all data)	R ₁ = 0.0295 wR ₂ = 0.0480	R ₁ = 0.0429 wR ₂ = 0.0619	R ₁ = 0.0287 wR ₂ = 0.0509	R ₁ = 0.0350 wR ₂ = 0.0711
Largest Diff Peak and Hole, e/Å ³	0.62 / -0.97	0.91 / -0.80	0.97 / -0.85	0.73 / -1.01

Table S2. SHAPE analysis for compounds **1-3**.

	HP	PPY	OC	TPR	JPPY
1	33.440	21.464	2.556	11.733	24.621
2	30.651	21.411	3.368	11.9961	24.288
3	34.524	21.375	2.835	9.436	25.884
4 (Dy1A)	36.196	17.823	4.991	8.050	22.397
4 (Dy1B)	35.268	15.540	6.261	6.614	19.958

HP: Hexagon
PPY: Pentagonal Pyramid

OC: Octahedron
TPR: Trigonal Prism
JPPY: Johnson Pentagonal Pyramid

Table S3. Fitting of the Cole-Cole plots with a sum of two generalized Debye functions under a zero dc-field for **1** in the temperature range 1.8-3.4 K.

T (K)	$\chi_{S\text{tot}}$	$\Delta\chi_1$	α_1	$\Delta\chi_2$	α_2
1.8	1.74813E-5	3.00748	0.53513	4.14098	0.30252
2.6	2.29322E-5	3.0192	0.61971	3.05994	0.2269
3.4	6.26249E-5	2.21852	0.58985	3.02116	0.31659

Table S4. Fitting of the Cole-Cole plots with a sum of two generalized Debye functions under a zero dc-field for **1** in the temperature range 4.2-5.8 K.

T (K)	$\chi_{S\text{tot}}$	$\Delta\chi_1$	α_1	$\Delta\chi_2$	α_2
4.2	1.13926	0.74529	2.27817E-8	2.47032	0.39651
5	1.07482	0.94937	2.22696E-8	1.74271	0.25781
5.8	0.92454	0.92129	8.12134E-8	1.5118	0.22107
6.6	0.85192	0.87944	1.38927E-7	1.2723	0.16111
7.4	0.60068	0.7933	1.63451E-7	1.35265	0.21485
8.2	0.17664	0.71221	7.00797E-7	1.63274	0.29722
9	0.00117	0.66031	1.37183E-6	1.67163	0.30663
9.8	0.00181	0.56631	2.11023E-6	1.59686	0.367
10	0.00227	0.57103	2.44404E-6	1.55074	0.37856
10.6	0.00281	0.52062	3.70545E-6	1.50054	0.41455
11	0.0034	0.50263	5.43333E-6	1.4384	0.35932
11.4	0.0048	0.46784	5.31582E-6	1.42342	0.39733
12	0.00561	0.4167	7.86266E-6	1.37402	0.38844
12.2	2.0557E-7	0.3809	1.58797E-5	1.39947	0.36148
13	4.7671E-7	0.20902	9.87394E-6	1.46957	0.24383

Table S5. Fitting of the Cole-Cole plots with a generalized Debye model under a zero dc field for **3**.

T (K)	χ_s	χ_T	α
1.8	4.80576	5.9026	0.39817
1.9	4.49632	5.60558	0.38874
2	4.35738	5.29468	0.39789
2.1	4.13023	5.02445	0.39849
2.2	4.02175	4.87347	0.40395
2.3	3.81128	4.62431	0.40076
2.4	3.66648	4.43693	0.4162
2.5	3.50906	4.24709	0.40465
2.6	3.39341	4.09027	0.40192
2.7	3.24128	3.93354	0.41594
2.8	3.15623	3.79894	0.35362
2.9	3.04335	3.65962	0.41914
3	2.94766	3.54677	0.42764
3.1	2.88498	3.39973	0.43122
3.2	2.76947	3.32669	0.45486
3.4	2.60484	3.13154	0.45247
3.6	2.46979	2.95857	0.39817
3.8	2.31684	2.80574	0.38874
4	2.21929	2.66672	0.39789

Table S6. Fitting of the Cole-Cole plots with a generalized Debye model under a zero dc field for 4.

T (K)	χ_s	χ_T	α
1.8	2.94468	5.13758	0.42509
2	2.73034	4.74524	0.42283
2.2	2.54542	4.40561	0.4162
2.4	2.34045	4.03003	0.41118
2.6	2.18024	3.73928	0.40807
2.8	1.84841	3.49187	0.43223
3	1.94703	3.28282	0.38903

3.2	1.92777	3.08464	0.34455
3.4	1.84922	2.91778	0.33955
3.6	1.76603	2.76529	0.33258
3.8	1.6877	2.6256	0.3295
4	1.73153	2.47704	0.25817

Table S7: Fit parameters of the temperature dependence of the relaxation time for **1** from a combination of Raman and QTM process (zero field) or Raman (1000 Oe).

Compound	n	$C (s^{-1} \cdot K^{-n})$	$\tau_{QTM} (s)$
1 (0 Oe)	6.62 ± 0.06	0.00046 ± 0.00008	0.0202 ± 0.006
1 (1000 Oe)	6.12 ± 0.09	0.0015 ± 0.0003	-

Table S8: Fit parameters of the field dependence of the relaxation time at 15 K for **4**

Compound	$D (s^{-1} K^{-1} Oe^{-4})$	$B_1 (s^{-1})$	$B_2 (Oe^{-2})$	K
4 (2 K)	2.66×10^{-11}	2676.53	3×10^{-4}	24.03

Table S9. Fitting of the Cole-Cole plots with a sum of two generalized Debye functions under a 1000 Oe dc-field for **1**.

T (K)	$\chi_{S\text{tot.}}$	$\Delta\chi_1$	α_1	$\Delta\chi_2$	α_2
4.2	1.02098	2.52682	0.00305	0.81069	0.40534
5	1.01306	1.80075	8.97045E-4	0.93247	0.46623
5.8	0.9254	1.48861	3.60262E-4	0.92838	0.46419
6.6	0.78456	1.36332	1.58842E-4	0.86529	0.43265
7.4	0.5553	1.40083	6.78429E-5	0.78802	0.39401
8.2	0.20641	1.58677	2.49393E-5	0.72842	0.36421
9	4.90936E-14	1.69376	1.04483E-5	0.63705	0.31853
9.5	5.92914E-14	1.62554	7.41641E-6	0.59823	0.29912
10	6.84606E-14	1.54999	4.71087E-6	0.57659	0.2883
10.5	7.8863E-14	1.48895	4.05468E-6	0.54691	0.27346
11	9.79336E-14	1.47491	2.56557E-6	0.49151	0.24576

11.5	8.7493E-14	1.3974	4.10967E-6	0.47339	0.23669
12	1.01225E-13	1.35158	4.80929E-6	0.44003	0.22002
13	2.14198E-13	1.3419	3.35608E-6	0.33939	0.1697

Table S10. Fitting of the Cole-Cole plots with a sum of two generalized Debye functions under a 1000 Oe dc-field for **4**.

T (K)	$\chi_{S\text{tot.}}$	$\Delta\chi_1$	α_1	$\Delta\chi_2$	α_2
1.8	0.55214	1.86687	0.55214	3.13122	0.03713
2.06	0.65521	1.98055	0.60916	2.46211	0.02685
2.33	0.54284	1.74712	0.5834	2.31935	0.0172
2.60	0.44246	1.92869	0.65521	1.7973	0.00934
2.86	0.34622	1.31105	0.44848	2.03688	0.00515
3.13	0.55214	1.3878	0.52624	1.66406	0.00296
3.40	0.65521	1.34566	0.54284	1.52975	0.00177
3.66	0.54284	1.22778	0.51038	1.4654	0.00111
3.93	0.44246	1.09761	0.49424	1.4418	7.11662E-4
4.30	0.34622	1.00565	0.44246	1.37359	4.79089E-4
4.45	0.55214	0.80091	0.6376	1.46698	2.68913E-4
4.73	0.65521	0.74062	0.37738	1.38808	2.25593E-4
5	0.54284	1.16865	0.34622	0.8647	1.94696E-4

References

- 1 N. F. Chilton, D. Collison, E. J. L. McInnes, R. E. P. Winpenny and A. Soncini, *Nat. Commun.*, 2013, **4**, 2551.